CHAPTER I
INTRODUCTION

1.1 Introduction

Zeolites are framework aluminosilicates, which have been widely used as molecular sieves and adsorbents for separation industrial, catalysts for catalytic cracking in petroleum refinery and ion-exchange resins due to their meso and microporous structures [Van Bekkum *et al.*, 1991, Dyer, 1988 and Ghobarkar *et al.*, 1999]. The framework structures of aluminosilicates occur from the joining of tetracoordinated SiO_4^{4-} with tetracoordinated AlO_4^{5-}. In general Al^{3+} ion favors to form in octahedral coordinate form as predicted from radius ratio [Barsoum, 1997]. Due to their high polarizing power, Al^{3+} and O^{2-} combination tends to increase the covalent characteristic of the bond and favor tetrahedral coordination. AlO_4^{5-} is negative charge as comparing with SiO_4^{4-} tetrahedral due to their tri-valent cations, therefore the charge of the whole framework is normally compensated by mono and/or di-valent cations within or close to the cavities, while additional water molecules are present in the framework cavities. The general chemical formula unit of zeolites is given in Equation (1.1).

$$M_{(m/z)}^{z+} \, [Al_m \cdot Si_n \cdot O_{2(n+m)}] \cdot qH_2O \qquad (1.1)$$
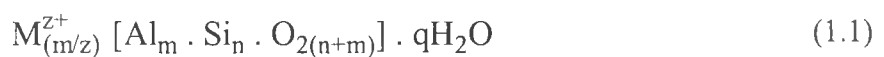
M : Extra framwork cations (e.g. Li^+, Na^+, K^+, etc.)
z : Charge of cations
m : Number of Al per formula unit
n : Number of Si per formula unit
q : Number of water molecules

The surface of the zeolites' framework is essentially oxygen atoms, as Si and Al are buried or recessed in the tetrahedral of oxygen atoms so they are not exposed and cannot be accessed by adsorbate molecules. The anionic oxygen atoms are also much more polarizable than the Al and Si cations, as well as being more abundant. Therefore the numerous and anionic oxygen atoms dominate the van der Waals

interaction, as illustrated in Figure 1.1. Beside the anionic oxygen, cations are located at certain sites. Four different positions of extra-framework cations of zeolites are possible [Gottardi *et al.*, 1985]. The first position is that, the cation is only coordinated by framework oxygens. For the second position, the cation is coordinated by framework oxygens at two nearly opposite side together with some water molecules. The third possible position is for the cation to be bounded one side with framework oxygen and the other side by water molecules. The other possible position is the completely surrounding of the cation by water molecules.

T = Silicon or Aluminum Atom

(a)   (b)
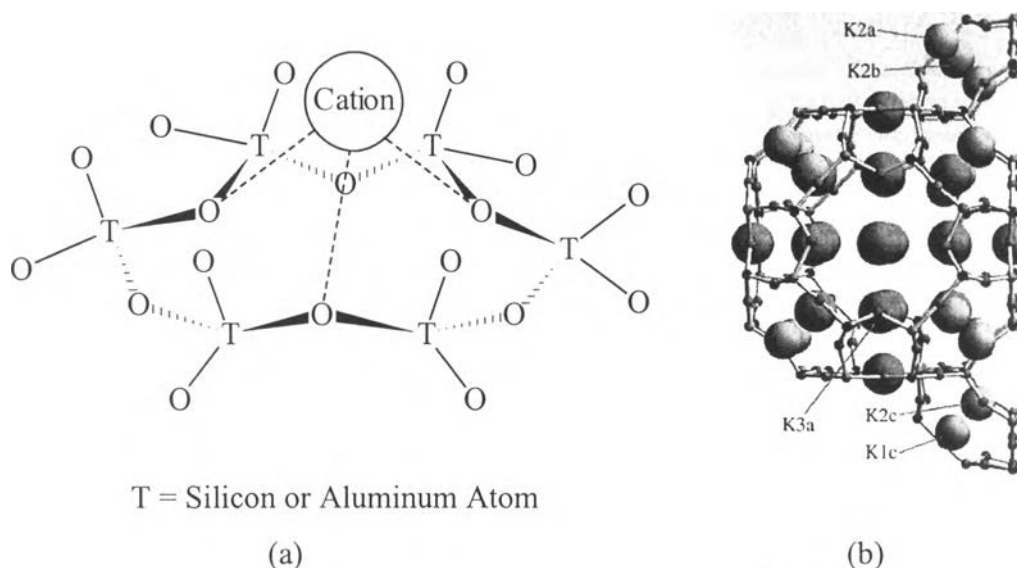
Figure 1.1 Cation site of six-membered ring zeolites (a); structure of K-LTA zeolite on the [100] direction (b) which shaded balls are K^+ ion. [Ikeda *et al.*, 2000]

The size of the windows depends on the number of oxygen atom in the ring. The aperture size as well as the adsorptive properties can be further modified by the number and type of exchanged cations. For example, Type A zeolites (or LTA) are synthesized in a sodium form (Type 4A or Na A zeolite) with 12 sodium cations occupying all eight sites with as effective aperture size of 3.8 Å. By replacing Na^+ ion with K^+ ion (Type 3A zeolite), effective aperture size is smaller due to the larger K^+ ion while replacing with Ca^{2+} or Mg^{2+} ion (Type 5A), the aperture size of the Type A zeolite increases since $2Na^+$ are replaced by one bivalent cation. The characteristics of the major commercial zeolite sorbents are given in Table 1.1.

Table 1.1   Characteristics of Major Synthetic Zeolite Sorbents [Ralph, 1997]

Zeolite Type	Major Cation	Nominal Aperture Size, Å	Bulk Density[a] lb/ft³
3A (Linde)	K	3	40
3A (Davidson)	K	3	46
4A (Linde)	Na	4	41
4A (Davidson)	Na	4	44
5A (Linde)	Ca	5	45
5A (Davidson)	Ca	5	44
10X (Linde)	Ca	8	40
13X (Linde)	Na	10	38
13X (Davidson)	Na	10	43

[a] Based on 1/16 inch pellets or beads

At least forty species of naturally occurring zeolites have been found. The principal ones are chabazite, gmelinite, mordenite, levynite, and faujasite. More than 150 types of zeolites have been synthesized; they are designated by a letter or group of letters; such as Type A, Type X, Type Y, Type ZSM, and so on. Chemical compositions of some important aluminosilicate zeolites were listed in Table 1.2.

The first known classification properties of zeolites were their exchange capability of extra-framework cations, depended on charge distribution of the zeolite framework caused by (Si,Al)-distribution together with the charge distribution within the void system and the possibility of reversible water absorption [Eitel *et al.*, 1966]. Within the zeolite structure, water molecules are present in the cavities (channels and cages) of the framework structure. Desorption of the binding water in zeolites, zeolitic water, is time- and temperature-dependent. Based on water desorption at various temperature, water loss under dynamic conditions shows the different crystallographic positions of water molecules in between the zeolite framework. The same behavior is observed under vacuum condition. Moreover, the unique ion exchange properties of zeolites are varied specifically dependent on the different crystallographic building principles [Barrer *et al.* 1953 and 1958].

Table 1.2 The chemical compositions of some important aluminosilicate zeolites [Gottardi *et al.*, 1985 and Naccache, 1984]

Na-zeolites

Zeolite code	Zeolite phase	Zeolite structure units	Molar ratio Na:Al:Si	Idealized chemical formular
CAN	Cancrinite	4 & 6	1:0.75:0.75	$Na_8[Al_6Si_6O_{24}]$ x 2(OH) x 2.66H_2O
SOD	Hydroxy-sodalite	4 & 6	1:0.75:0.75	$Na_8[Al_6Si_6O_{24}]$ x 2(OH) x 2H_2O
LTA	Zeolite LTA	4 & 4-4	1:1:1	$Na_{12}[Al_{12}Si_{12}O_{48}]$ x 27H_2O
EDI	Zeolite F	4 = 1	1:1:1	$Na_5[Al_5Si_5O_{20}]$ x 9H_2O
LTN	Zeolite N, NaZ 21	4 & 6	1:1:1	$Na[AlSiO_4]$ x 1.1H_2O
FAU	Na-zeolite X	6-6	1:1:1.4	$Na_5[Al_5Si_7O_{24}]$ x 9H_2O
NAT	Natrolite	4=1	1:1:1.5	$Na_{16}[Al_{16}Si_{24}O_{80}]$ x 16H_2O
GIS	Gobbinsite	4-ring	1:1:2.2	$Na_5[Al_5Si_{11}O_{32}]$ x 11H_2O
GME	Gmelinite	6 & 6-6	1:1:2	$Na_2[Al_2Si_4O_{12}]$ x 5H_2O
ANA	Analcime	4 & 6	1:1:2	$Na_{16}[Al_{16}Si_{32}O_{96}]$ x 16H_2O
KFI	Zeolite ZK 5	4 & 6-6	1:1:2.2	$Na_{30}[Al_{30}Si_{66}O_{192}]$ x 98H_2O
CHA	Na-chabazite	6-ring	1:1:2.22	$Na_{3\,72}[Al_{3\,72}Si_{8\,28}O_{24}]$ x 9.7H_2O
FAU	Na-zeolite Y	6-6	1:1:2.76	$Na_{51}[Al_{51}Si_{141}O_{348}]$ x 7.83H_2O
EAB	Zeolite TMA	4 & 6	1:1:2.83	$Na_{9\,4}[Al_{9\,4}Si_{26\,6}O_{72}]$ x 36.8H_2O
ERI	Erionite	4 & 6	1:1:3	$Na_9[Al_9Si_{27}O_{72}]$ x 27H_2O
HEU	Na-heulandite	4-4=1	1:1:3.04	$Na_{8\,9}[Al_{8\,9}Si_{27\,1}O_{72}]$ x 26H_2O
STI	Barrerite	4-4=1	1:1:3.5	$Na_8[Al_8Si_{28}O_{72}]$ x 26H_2O
MOR	Na-mordenite	5-1	1:1:5	$Na_8[Al_8Si_{40}O_{96}]$ x 24H_2O
MEL	Zeolite ZSM 11	5-1	1:1:11	$Na_8[Al_8Si_{88}O_{192}]$ x 16H_2O
MFI	Zeolite ZSM 5	5-1	1:1:86.27	$Na_{1\,1}[Al_{1\,1}Si_{94\,9}O_{192}]$ x 2.36H_2O

Zeolites are high capacity, selective adsorbents capable of separating molecules based on the size and shape of the molecule relative to the size and geometry of the main apertures of the structure. Separation may be based on the molecular-sieve effect (Figure 1.2) or may involve the preferential or selective adsorption of one molecular species over another. Separations are governed by several factors. The basic framework structure or topology of the zeolite determines the pore size and the void volume. The exchange cations, in terms of their specific location in the structure, their population density, their charge and size, affect the molecular-sieve behavior and adsorption selectivity of zeolite.
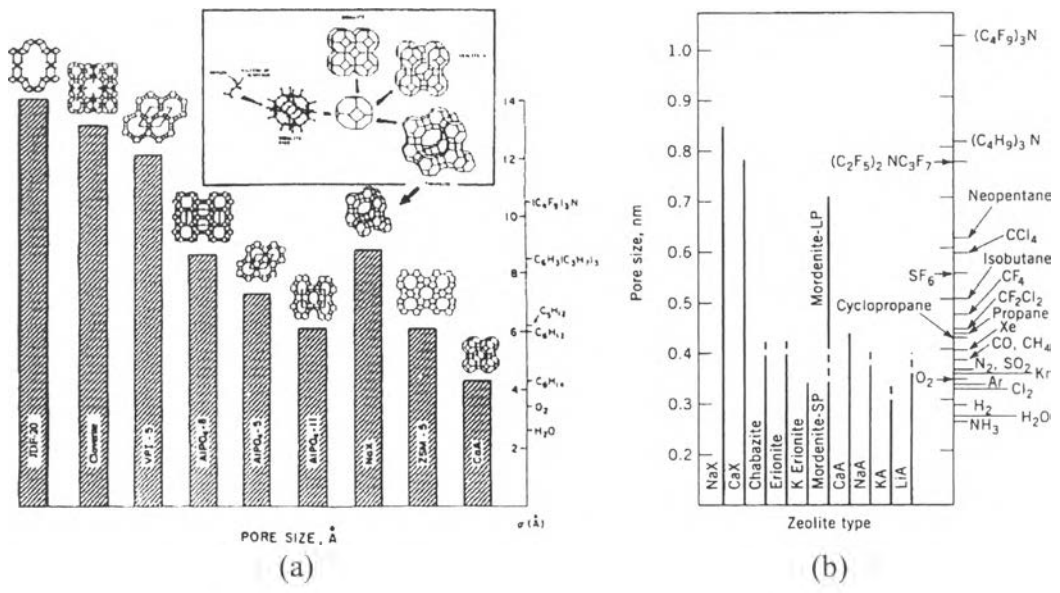
Figure 1.2 Correlation between pore size of molecular sieves and the kinetic diameter of various molecules with pore size of molecular sieves in range of 4 – 14 Å (a) [Davis, 1993] and 4 - 8.5 Å (b) [Breck, 1974]

The zeolites of most interest in catalysis are those having medium to large pore size, containing 10- or 12-ring oxygen atoms, and having relatively high Si/Al ratio. Dissociation of water forms a hydorxyl group on the aluminum atom. The resulting structure, in which the aluminum and the silicon are both tetrahedrally coordinated, is Brönsted acid (having ability to donate a proton) [Satterfield, 1991]. As this structure is heated, water of constitution is driven off and Brönsted acid are converted to Lewis acid (having ability to accept an electron pair) sites, as shown in scheme I. On the other hand, addition of water and heating can convert Lewis acid sites back to Brönsted acid sites. Aluminum atom is electrophilic and can react with hydrocarbons to form an adsorbed carbenium ion, as illustrated in scheme II for the two types of sites.

Bronsted acid   Lewis acid
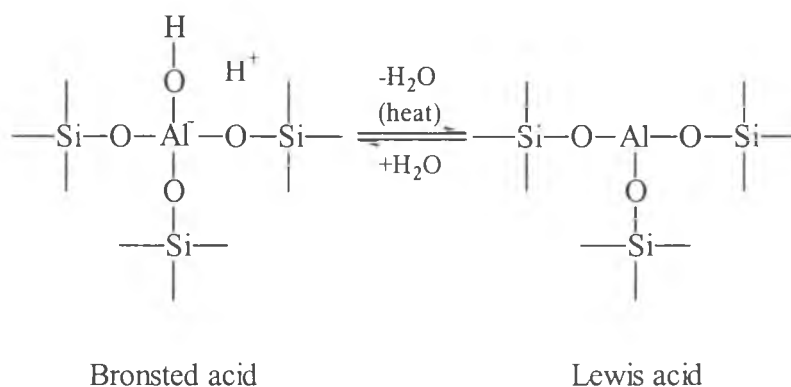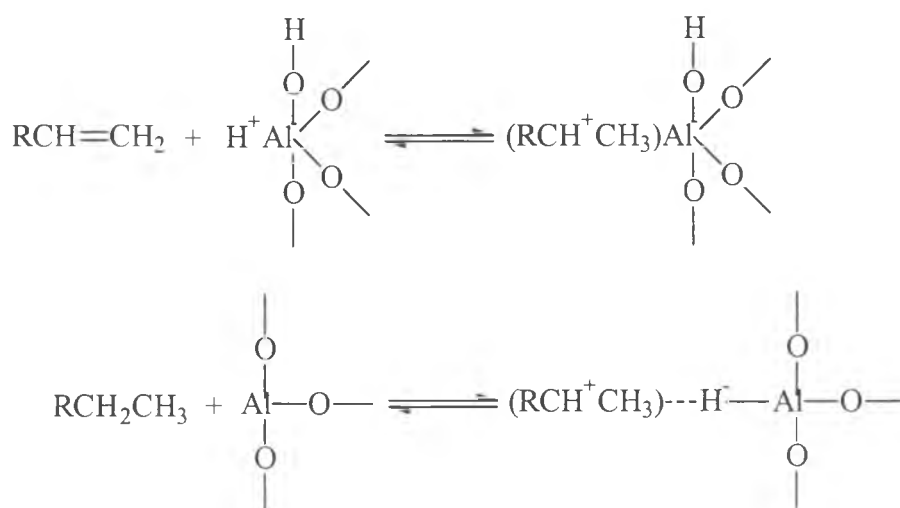
Scheme I

Scheme II

Zeolites of high current interest industrially are zeolite Y and mordenite which have a 12-ring system, and ZSM-5, which has a 10-ring system. Acidity site and/or strength can be measured by Hammet indicators, TPD of adsorbed ammonia, TPD of alkylamines and microcalorimetry with acidity strength determined by structure, coordination and partial charge on the surface (enthalpy change of neutralization of a base). Total-acidity determined by the density of acid site on the catalyst surface, is called acid density. Table 1.3 showed the example of physicochemical characteristics of ZSM-5 additive at various Si/Al ratios measured by TPD of ammonia [Triantafillidis *et al.*, 1999]. The strong acid sites were responsible for alkylation reaction, while olefin oligomerization mainly occurred on the weak Brönsted acid [Corma *et al.*, 1994]. In order to avoid the olefin

oligomerization, the high ratio of stronger to weaker Brönsted acid sites is necessary.

Table 1.3   Physicochemical characteristics of zeolite ZSM-5 samples [Triantafillidis *et al.*, 1999]

Si/Al ratio (C.A.)[a]	Surface area (m²/g, SP BET)[b]	No of acid sites (mmol of NH₃/g of zeolite, TPD)			Particle size (μm, SEM)
		Total	Weak	Strong	
12.5	431	1.15	0.55	0.60	10 – 15
25	476	1.05	0.51	0.54	0.5 – 2
35	448	0.70	0.34	0.36	10 – 30
>1000	430	0.07	0.07	0	10 – 15
28	437	0.89	0.42	0.47	0.5 – 2
41	439	0.68	0.34	0.34	0.5 – 2

[a] Chemical analysis

[b] Single-point BET method

1.1.1   Classification of Zeolites

The extraordinary properties of zeolites are caused by their crystal lattice. A proper classification starts from the 3-dimensional bonding of the tetrahedrally coordinated framework cations. The connection of $(SiO_4)^{4-}$ and $(AlO_4)^{5-}$ tetrahedral causes myriad of lattice architectures which consist of channels and cages with different types of connection as illustrated in Figure 1.3. The arrangement of tetrahedral (primary building units) can be classified into various types of secondary building units (SBUs) as illustrated in Figure 1.4 [Ertl *et al.*, 1997]. Each SBU connects in the way that the cylinders or pore are built in different cages model (periodic building units, PBUs), as shown in Figure 1.5, while the unit cell of each structure type is formed from the connection of each PBU as some shown in Figure 1.6. Hence the proper classification of zeolites is based on their crystal lattices.

Each unit cell structure is coded in three capital letters, called structure type code, by following the rules set up by an IUPAC Commission on Zeolite Nomenclature in 1978 [Barrer, 1979]. The codes are generally derived from

the name of the type of materials and do not include the numbers and characters other than capital roman letters. All structure types published up to April 2000 are listed in Table 1.4 [Baur *et al.*, 2000].
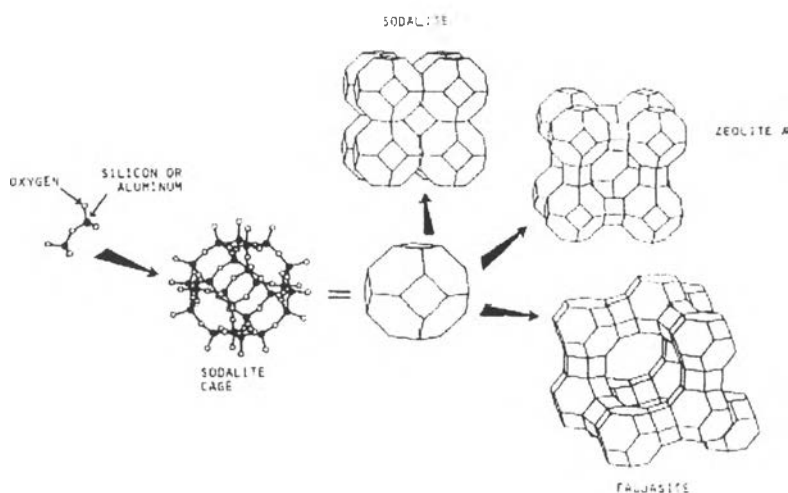
Figure 1.3   Schematic of zeolite frameworks.   The synthetic faujasites are zeolites NaX and NaY (difference between NaX and NaY is the Si/Al $\cong$ 1.1, NaY $\cong$ 2.4) [Davis, 1991]
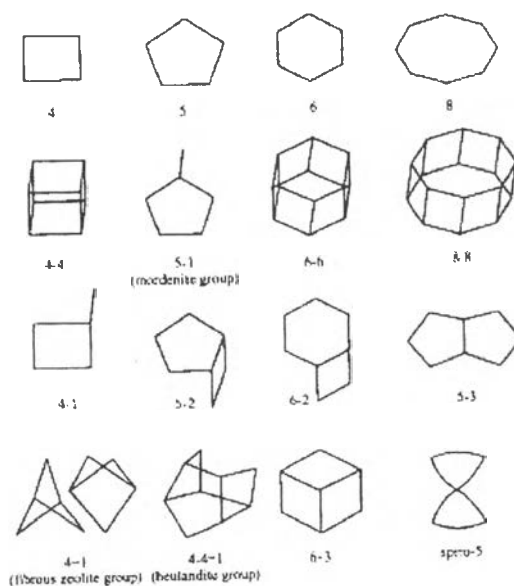
Figure 1.4   Different secondary building units (SBUs) of today known zeolite structures [Ghobarkar *et al*, 1999]
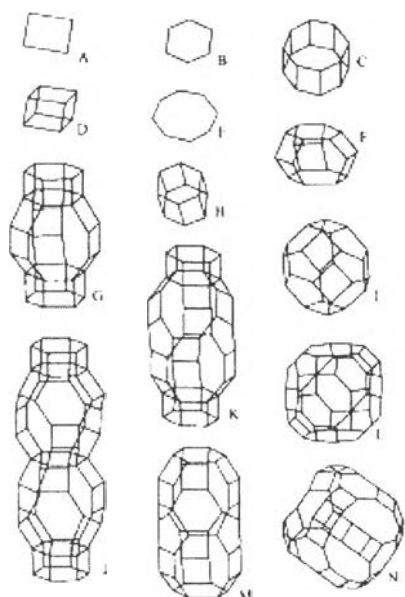
Figure 1.5 Selected zeolite cages: A = 4-ring (window opening to cage of infinite length); B = 6-ring (window opening to cage of infinite length); C = 8-8-cage (δ-cage); D = 4-4-cage; E = 8-ring (window opening to cage of infinite length); F = cancrinite cage (ε-cage); gemlinite cage (γ-cage); H = 6-6-cage; I = sodalite cage (β-cage); J = levyne cage; K = chabazite cage; L = α-gage; M = erionite cage; N = faujasite supercage [Ghobarkar *et al.*, 1999]

(a)   (b)
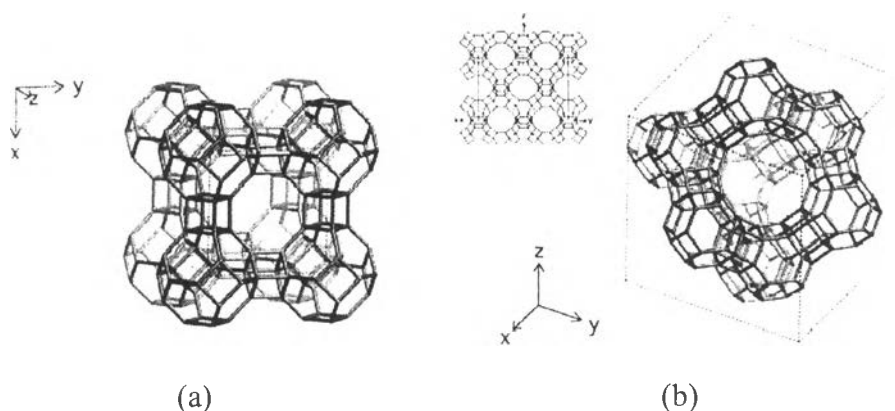
Figure 1.6 Line representation of unit cell structures: (a) type A zeolite or LTA and (b) type X and Y or faujasite [Baerlocher *et al.*, 2001]

Normally, zeolite type silicates and phosphates apparently constitute two distinctive categories of micorporous materials. However, Table 1.4 also show, there are three rather than two distinct groups of framework types that apart from those associated with silicates and phosphates there is a sizable group of structure types which have been found to occur both in silicates and phosphates.

Zeolites and zeolite like material (porous frameworks) can also be distinguished from non-zeolite framework structures (denser frameworks) like tectosilicates by their framework density (FD), defined as number of tetrahedrally coordinated atom (T-atoms) per 1000 Å^3, which is always lower than FD for normal

tetrahedral framework structures. This is caused by the channel and cage system [Meier *et al.*, 1996 and Baerlocher *et al.*, 2001]. A characteristic gap between zeolite structure types and nonporous framework structure types exists in range from 19 to over 21 T-atoms per 1000 Å^3, depending on the type of smallest rings present, as shown in Figure 1.7. This fact can be used for the independent control of a structure type to be classified as zeolite, although no correlation between framework density and cavity (channel or cage) diameter exists.

Table 1.4   Microporous zeolite-type materials [Baur *et al.*, 2000]

Silicates[a]			Both Silicates and Phosphates	Phosphates[b]	
AFG	IFR	OFF	ABW	ACO	SAO
ASV	ISV	OSO	AET	AEI	SAS
*BEA	ITE	-PAR	AFI	AEL	SAT
BIK	JBW	PAU	AFX	AEN	SAV
BOG	KFI	-RON	ANA	AFN	SBE
BRE	LIO	RSN	AST	AFO	SBS
CAS	LOV	RTE	BPH	AFR	SBT
CFI	LTN	RTH	CAN	AFS	VFI
-CHI	MAZ	RUT	CGS	AFT	WEI
CON	MEI	SFE	CHA	AFY	ZON
DAC	MEL	SFF	DFT	AHT	
DDR	MEP	SGT	EDI	APC	
DOH	MFI	STF	ERI	APD	
DON	MFS	STI	FAU	ATN	
EAB	MON	STT	GIS	ATO	
EMT	MOR	TER	LAU	ATS	
EPI	MSO	TON	LEV	ATT	
ESV	MTF	TSC	LOS	ATV	
EUO	MTN	VET	LTA	AWO	
FER	MTT	VNI	LTL	AWW	
FRA	MTW	VSV	MER	CGF	
GME	MWW	-WEN	PHI	-CLO	
GON	NAT	YUG	RHO	CZP	
GOO	NES		SOD	DFO	
HEU	NON		THO	OSI	

[a] Including germanates

[b] Including arsenates
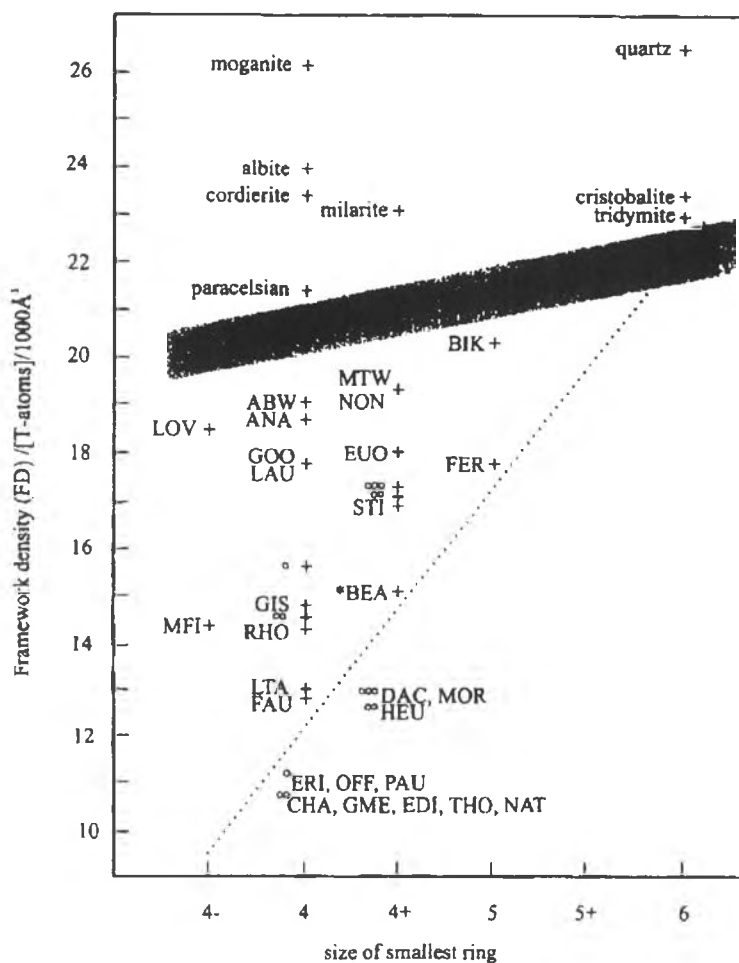
Figure 1.7 Framework density of selected zeolites in respect to normal tectosilicates [Meier *et al.*, 1996 and Baerlocher *et al.*, 2001]

1.1.2 Zeolite Synthesis

Most zeolites used come from either nature or synthesis. Synthetic zeolites are obtained via the sol-gel process which amorphous gel is produced from an interaction between aluminate and silicate or silica sol. The sol-gel process undergoes two main steps, hydrolysis and condensation reactions [Ertl *et al.*, 1997].

Hydrolysis   :   M-OR + H$_2$O $\longrightarrow$ M-OH + RO-H   (1.2)

Condensation :   M-OH + X-OM $\longrightarrow$ M-O-M + X-OH   (1.3)

x = H or R

The mechanisms of these two reactions in acid and base were different as illustrated in Scheme III [Wright, 2001].

Hydrolysis Mechanism:

Acid Catalyzed;
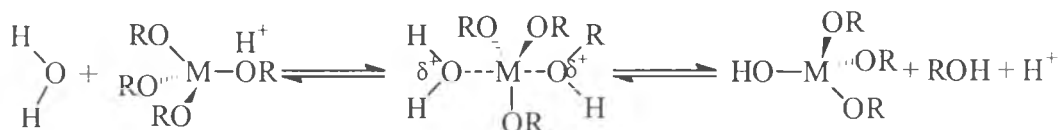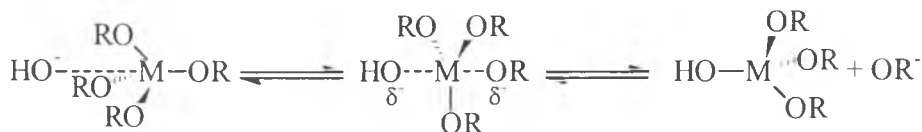
Base Catalyzed;

Condensation Mechanism:

Acid Catalyzed;
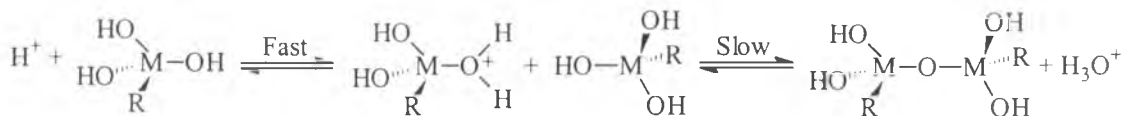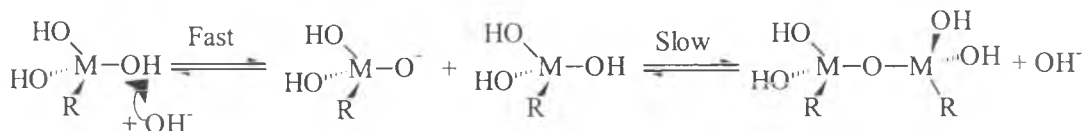
Base Catalyzed;

Scheme III

The rate trends in acid and base catalyzed processes for successive hydrolysis of the four alkoxy groups around metal can be described in term of electronic effects. Alkyl groups are more electron donation group than hydoxy group. Thus for the positively charged transition state of the acid-catalyzed reaction, which more alkoxy groups are replaced by hydroxy groups, the transition state becomes less stabilized and the reaction rate decreases. Conversely, for the

negatively charged transition state of the base-catalyzed reaction, more OH groups mean more stabilization of the transition state and faster reaction. Similar arguments obviously show that the reverse esterification reaction rate are more likely in acidic conditions, where esterification stabilizes the transition state, than in basic conditions.

A three-dimensional gel network comes from the condensation of partially hydrolyzed species in which the degree of gelation impacts on the properties of the product. At the hydrolysis rate faster than the condensation rate. the results obtained give weakly branch, while in the opposite direction, resulting gel is highly branched and contains colloidal aggregates.

To obtain any crystalline phase, further hydrothermal treatment is need. It can be processed by either conventional or microwave heating. In both systems, the amorphous gel undergoes continual dissolution and reconstruction and crystalline phase grows [Bell, 1999, Barrer, 1983 and Szostale, 1985] under hydro-pressure. However, the nucleation rate in both cases is different. For conventional heating, transferring heat from the generation source to media or materials deals with heat transfer coefficient of each material, causing convection current of heat or non-homogeneous heat distribution. As a result, the nucleation rate is very fast at the area of high temperature and very low at low temperature region.

Microwave heating attributes fast homogeneous nucleation and easy dissolution of the gel due to the fast homogeneous heating and the formation of active water molecules [Jansen *et al.*, 1992]. It is a fast and energy efficient technique, which prevents other side reactions owing to their nature in interaction caused from dielectric property of each materials [Cundy, 1998]. The interaction reaction of dielectric materials under microwaves leads to the dielectric heat generated from electric dipole response in the applied electric field of microwave [Xu *et al.*, 2000]. When the dipolar reorientation is unable to respond to the alternating electric field's frequency, a phase lag occurs, giving rise to a polarization current which is in phase with the applied field. As a consequence, rapid heating occurs in the medium. From the dipole rotation frequency, materials, which the dipoles rotate freely, such as liquid, establish the dissipation of energy from the applied field, and for ionics the dissipative energy occurs by oscillation.

In simplifying the method of calculation, the single mode irradiation condition is used for study. The heating rate (dT/dt) is formulated based on single-mode resonant cavity of microwave application as illustrated in Equation 1.4. The experimental and the model predicted temperatures vs. power plot obtained under single mode irradiation conditions of a few ceramics are shown in Figure 1.8. The coupling of material with microwave frequency is possible in the case that material has dipolar absorption in the same region as reactor frequency. The coupling starts to occur when the natural frequency of material equals to given frequency. However, if the relaxation frequency of the material match with frequency of reactor and the dipole relaxation times are affected by temperature ($\tau(T)$), the microwave absorption of the material will be optimally increased. This can be achieved by varying the reactor frequency itself or the temperature ($\in(\omega, \tau(\mathbf{T}))$). In the case of material, which has dielectric loss peak frequency higher than the microwave reactor frequency, the initial microwave heating shifts higher as a result microwave coupling decreases and further heating stops. The choice of materials for microwave application is evaluated base on above considerations.
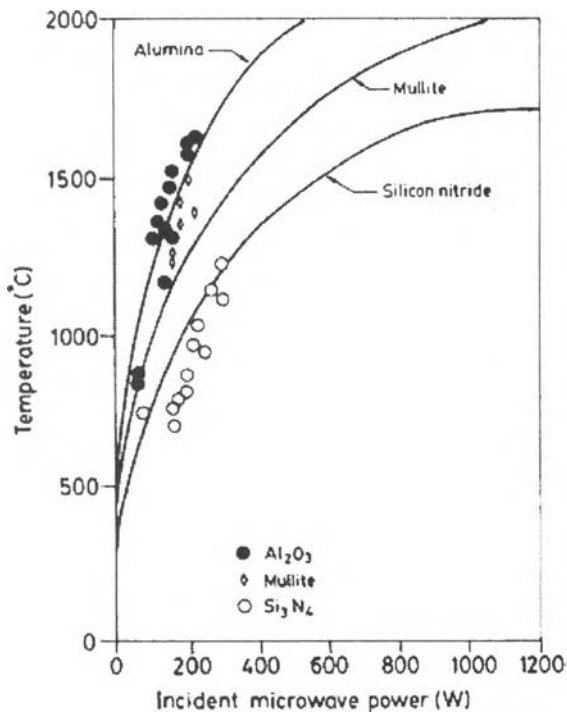
Figure 1.8 Steady-state temperature vs. power plots for three different ceramics under single mode irradiation conditions. Solid lines were calculated from equations 1.4 for heating rate in a single-mode resonant cavity. [Xu *et al.*, 2000]

Microwave coupling's ability mostly depends on the dielectric properties of material which are dependent on both the chemical composition, such as impurities, aliovalent substitution and chemical nature of material, and the physical state of material, for example, surface defects, surface charge and polarization. Interaction of material with microwave can be classified into there categories; microwave reflectors, such as metals and alloys which are used for microwave guides, microwave transmitters, such as fused quartz, zircon, several glasses, ceramic (not containing any transition metal) and Teflon used for making cookware and containers, and microwave absorbers, that can take up energy from the microwave field and get heated up very rapidly. Many inorganic materials couple strongly to microwave at ordinary temperature, as listed in Table 1.5.

Table 1.5   Microwave-Active Elements, Nature minerals and Compounds [Xu *et al.*, 2000]

Element/mineral/ compound	Time (min) of mocrowave esposure	T, K	Element/mineral/ compound	Time (min) of mocrowave esposure	T, K
Al	6	850	NiO	6.25	1578
C (amorphous, <1 m)	1	1556	V_2O_5	11	987
C (graphite, 200 mesh)	6	1053	WO_3	6	1543
C (graphite, <1 m)	1.75	1346	Ag_2S	5.25	925
Co	3	970	Cu_2S (chalcocite)	7	1019
Fe	7	1041	$CuFeS_2$ (chalcopyrite)	1	1193
Mo	4	933	$Fe_{1-x}S$ (phyrrhotite)	1.75	1159
V	1	830	FeS_2 (pyrite)	6.75	1292
W	6.25	963	MoS_2	7	1379
Zn	3	854	PbS	1.25	1297
TiB_2	7	1116	PbS (galena)	7	956
Co_2O_3	3	1563	CuBr	11	995
CuO	6.25	1285	CuCl	13	892
Fe_3O_4 (mgnetite)	2.75	1531	$ZnBr_2$	7	847
MnO_2	6	1560	$ZnCl_2$	7	882

Because of their specific nature in interaction with microwave and heat generation from molecular level, fast homogeneous heating and formation of active water molecule introduce quick dissolution of inorganic gel and fast homogeneous nucleation. They cause shorten in synthesis time, high purity product and work well with broad composition. The produced particles are very small in size and have narrow particle size distribution.

$$\frac{dT}{dt} = \frac{4}{\tan\delta} \frac{1}{\rho C} \frac{\epsilon''}{\sqrt{\epsilon'}} \frac{1}{V_c} P_o \frac{\xi S}{\rho C} \left(\frac{area}{volume} \right)_{sample} (273 + T)^4 \qquad (1.4)$$

$\epsilon = dielectric\ constant$

$\delta = phase\ lag$

$\rho = mass\ density\ of\ the\ sample$

$V_c = cavity\ volume$

$P_o = microwave\ power\ inside\ the\ cavity$

$C = specific\ heat\ capacity\ of\ material$

$S = the\ Stefan - Boltzmann\ constant$

$\xi = surface\ emissivity\ of\ the\ sample$

Debye Equations:

$$\epsilon' = \epsilon_\infty + \frac{\epsilon_s - \epsilon_\infty}{1 + \omega^2 \tau^2} \qquad (1.5)$$

$$\epsilon'' = \frac{\epsilon_s - \epsilon_\infty}{1 + \omega^2 \tau^2} \qquad (1.6)$$

$\epsilon' = absorption\ frequency\ dielectric$

$\epsilon'' = relaxation\ frequency\ dielectric$

$\epsilon_s = zero\ frequency\ dielectric\ constant$

$\epsilon_\infty = infinite\ frequency\ dielectric\ constant$

$\omega = frequency\ of\ applied\ field$

$\tau = characteristic\ relaxation\ time$

1.2 Background and Literature Review

According to their great utilities in all aspects of human activities, zeolites, aluminosilicates or porous materials created by nature or by synthetic design are impressive in structuring design. Zeolite formation deals with a complex mechanism. A large number of reaction species, numerous polymerization and depolymerization of metal oxide are all involved in the process. To understand the crystallization process, Caputo *et al.* (2000) monitored zeolite synthesis system using Dynamic Light Scattering (DLS), X-ray diffraction (XRD) and Scanning electron microscopy (SEM) to follow in situ zeolite A crystallization. For non aged solution, the formation of a precursor phase (amorphous gel like) was observed. DLS results also indicated the sedimentation of particles soon after nucleation, causing non-uniform growth conditions and subsequently promoting secondary nucleation in the solution.

Schmacht *et al.* (2000) used ultrasonic wave for monitoring in real time synthesis of both zeolite A and zeolite X. Gel formation state prior to crystallization was also observed. Moreover, it was also found that some zeolite crystallization started earlier for aged reaction fluids.

Even the starting material for zeolite synthesis was changed to coal fly ash (Murayama *et al.*, 2002), the mechanism of zeolite synthesis was passed through the formation of amorphous gel before converting to the crystalline aluminosilicate. They also reported that the hydorxyl concentration in the alkali solution remarkably contributed to the dissolution step of SiO_4^{4-} and AlO_4^{5-} anion and the total rate of zeolite synthesis mainly depended on sodium cation concentration in the alkali solution. When sodium and potassium cations coexisted in the alkali solution of the hydrothermal reaction, the crystallization rate decreased with an increase in potassium cation concentration.

Alkali cations type and alkalinity of the system have highly influence on the zeolite synthesis. Kooli *et al.* (2002) and Zones *et al.* (1996) reported that alkalinity could dominate the silicate and aluminosilicate chemistry, hence playing a critical role in determining what product would be formed, while the alkali cations acted as template or structure-directing role and dominated the course of crystallization.

However, there is one work reported by Gittleman *et al.* (1996) that the alkali cations did not appear to server as templates or void filler during zeolite crystallization, nor did they stabilized soluble silicate or aluminate anion which served as building block during zeolite crystallization. The alkali cation appeared to regulate the transformation of the amorphous synthesis gel into crystalline material. They affected the rate of aluminosilicate dissolution, which affected the degree of polymerization of silicate and aluminate anions and the structure of aluminosilicate gel. Sodium cation served as bridging agent to connect silica particles into a denser gel where as the larger potassium, rubidium or cesium cations formed double layer around the silica particles thus hindering aggregation.

Machado *et al.*'s work (1999) also indicated that an upper limit for the incorporation of silica in MFI type framework (Si/Al = 12 – 29) was observed regardless of the silica-to-alumina raio of the starting gel (Si/Al = 18 – 20).

Using long-chain quaternary ammonium surfactant (organocations) as structural directing agents (act as guest molecules in the crystallization product) was invented for silica-based mesoporous material, non-silica-based mesostructured and/or mesoporous oxides so called "supramolecular templating method". David (1996) indicated that the organic species structure-directing agent dictated the final outcome of a zeolite synthesis, as illustrated in Figure 1.9. Firstly, the hydrophobic hydration sphere of tetrapropyl ammonium cations (TPA$^+$) was partially or completely replaced by silicate species. Favorable Van der Waals contacts between the alkyl groups of the TPA+ and the hydrophobic silicate species likely provided the enthalpic driving force while release of water to the bulk aqueous phase provided an additional enthalpic driving force for the assemble process, silylation methods. The organic-inorganic species then combined to form entities of size around 5 - 6 nm. These nanostructured entities were proposed to be the nucleation sites for crystal growth. The importance of this type of synthesis was the inorganic species organized by the organic molecules via numerous noncovalent, such as weak interaction, that ultimately determine the kinetic pathway of the crystallization process. Thus zeolite synthesis employed relatively weak noncovalent intermolecular interactions to direct the synthesis, the size and shape of structure-direction molecules correlating with the void dimension (Figure 1.10).
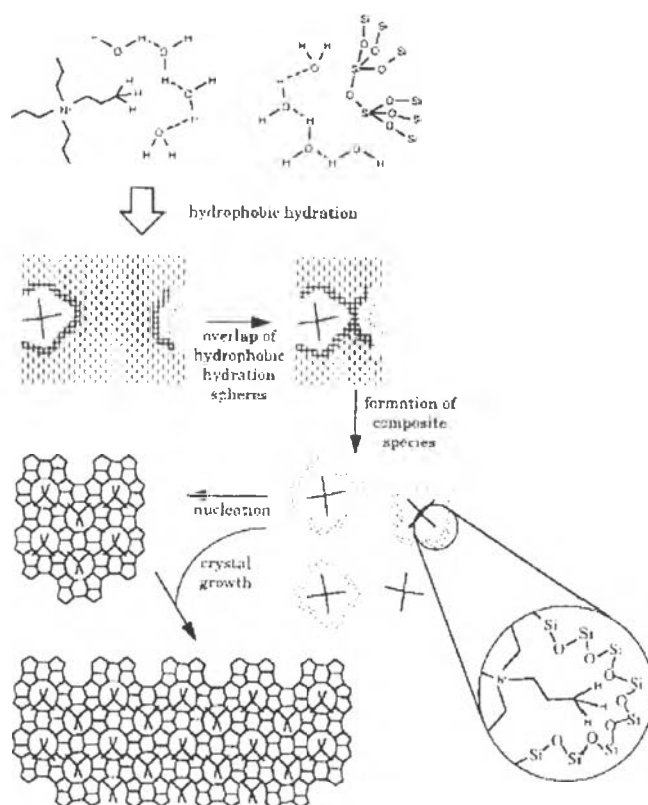
Figure 1.9 Schematic of proposed mechanism for the synthesis of ZSM-5 [Davis *et al.*, 1996 & 2000]
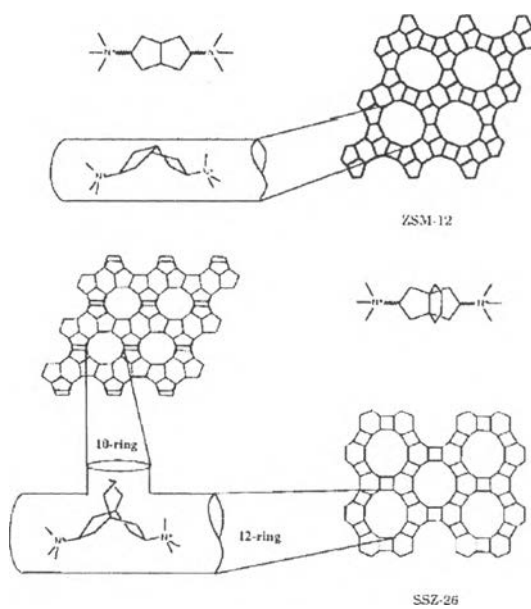
Figure 1.10 Schematic representations of organic structure-directing agents and zeolite formed [Davis *et al.*, 1996 & 2000]

Koegler *et al.* (1997) worked on synthesizing Si-ZSM-5 (MFI type) zeolite using tetrapropyl ammonium cations (TPA$^+$ cations) as a template. They indicated that nucleation and crystal growth occurred at the interface of gel particles and liquid where silicon source and template were present in abundance. Alkali ion at the surface may adversely affect zeolite nucleation by preferential attachment to the silica surface.

Shen *et al.* (1997) studied thermodynamics of ZSM-11 synthesis from amorphous silica and aqueous solution of tetraalkyl ammonium hydroxide (TAAOH). Both TPA+ and tetrabutyl ammonium cations (TBA$^+$ cations) were considered as the structure-directing agents, and calculation was performed for occlusion of either three or four TAA+ cations per unit cell of zeolite. Estimation of the change in internal energy and Gibbs free energy revealed that the synthesis of ZSM-11 should be favored by the occlusion of three TBA$^+$ cations per unit cell. The interaction of OH$^-$ anions with the zeolite framework to form defects in the form of siloxy groups (Si-O$^-$) was also considered in this study. Siloxy group must be formed to accommodate three or four occluded TAA+ cations per unit cell of ZSM-11.

Bell (1999) used Nuclear magnetic resonance (NMR) to determine the conformation in each state of synthesis. It was found that, for NaY and silicate (ZSM-5) synthesis, ^{29}Si-NMR indicated the changes in the connectivity of Si-atom breaking and reforming of the siloxane bonds during the aging and subsequent heating of gel state. In the presence of TPA$^+$ cations, ^{1}H-^{29}Si and ^{1}H-^{13}C cross-polarize magic angle spinning (CP-MAS NMR) evidenced that TPA$^+$ cations were occluded prior to the onset of silicate crystallization, which made the conformation change in the proper groups, providing more stable silicatlite state, thus giving rise to the rapid increase in the present crystallinity. The result also showed that TPA$^+$ cations were occluded into the channel intersections of silicate with one TPA+ being occluded per channel intersection.

Van der Puil *et al.* (1999) also used TPA$^+$ for MFI and BEA type zeolite synthesis coating on α–alumina beads and extrudates. It was found that low surface area supporters were essentially stable under zeolite synthesis conditions while high surface area supporters gave rise to dissolution of aluminum and coating instability.

Pretreatment of the supporters with the template resulted in an improved surface coverage by crystallite in sodium-rich zeolite synthesis. However, by testing on transalkylaltion of benzene with diethylene and alkylation of benzene with ethylene, coating catalyst did not show any better evident than that of unsuported catalyst.

De Moor *et al.* (2000) studied effect of template using TPA^+ cations, bis (tripropyl ammonium) hexamethylene dihydroxide (dimer of TPA^+) and bis (tripropyl ammonium-N-N'-hexamethylene)-N", N"-dipropyl ammonium trihydroxide (trimer of TPA^+) as structure-directing agents on Si-MFI synthesis. By using X-ray diffraction (SAXs, WAXs and USAXs modes), the formation of 2.8-nm-sized primary unit was observed upon dissolution of the silica source. The aggregation of these nanometer-scale primary units to 10-15-nm-sized particles was found to be an essential step in nucleation. Primary units of MFI were independent on the structure-directing agent used and the synthesis parameters, such as alkalinity, silica source and temperature. The organic species also did have a pronounced influence on the crystal growth step, rate size and morphology. The longer the organic part the slower in crystal growth rate and crystal size.

Based on the previous work using tetraalkyl ammonium cations, TPA^+ and TPA^+ derivatives are successfully used as structural directing agents for silica-based zeolite synthesis. However, they are incorporated in the framework and required the template-removing step (calcination at high temperature).

Other designed templates for Si-based zeolite synthesis are also studied. Linear triamine (N,N,N',N',N"-pentamethyl diethylene triamine) and its quaternary cations were used for ZSM-39 and ZSM-51 synthesis by Moini *et al.* (1997). The results have closely shown that the starting template was not intact in the zeolite framework. Only tetramethyl ammonium and trimethyl ammonium cation-speices, causing from decomposition of starting templates due to nucleophilic attack at α position or more likely proton abstraction at β position (Hofmann elimination), encapsulated in the zeolite cavities.

Small amines are also applied as structural directing agent for zeolite synthesis. Rollman *et al.* (1999) used certain noncyclic amines in the formation of 10-rings (ZSM-22 and ZSM-23) and 12-rings (ZSM-12) zeolite. At $SiO_2/Al_2O_3 =$

200, using ethylmethylamine and diethylamine provided highly crystalline structure as ZSM-22 while ethylamine and isopropylamine gave ZSM-23 products. Using larger size amine and cyclic amine can obtain ZSM-12, however, several amines, like n-propylamine played non-structure-specific pore and pH-stabilizing roles, and yielded ZSM-5. Changing SiO_2/Al_2O_3 to 40, effect of amines on crystalline formation also changed the ability of an amine to direct crystallization to one framework. Both size and shape of organic and alumina content of reaction mixture were all critically important. Moreover, The zeolite products were fully pore-filled with amine and low in Na (Na/Al < 1).

Rollman *et al.* (2000) also used alkylamines and polyamines for Si-based zeolite synthesis at SiO_2/Al_2O_3 ration below 40. Using C2-, C3- or C4-alkylamines provided ZSM 5 at the SiO_2/Al_2O_3 ration ~20. C3- and C4-alkylamines also gave ZSM-35 at SiO_2/Al_2O_3 ration between 20 – 40, while tert-butylamine also delivered MOR type zeolite. Polyamine as diethylene triamine and triethylene tetramine also dispensed ZSM-5 at SiO_2/Al_2O_3 ration below 20. Despite the very high pH of the crystallizaitons, all of products contained charge-balancing protonated amine and were low in Na content (Na/Al < 1).

DeLuca *et at.* (2001) also used tetraalkyl ammoium (TAA$^+$) cations; tetramethyl ammonium (TMA$^+$), tetraethyl ammonium (TEA$^+$) and tetrabutyl ammonium (TBA$^+$) cations , in synthesizing crystalline zeolites in low water content system. In the presence of non-organic template, mordenite (MOR) was obtained while in the system of TMA$^+$ cation sodalite (SOD) was produced. TEA$^+$ system provided mordenite and ZSM-5 (MFI) in larger crystal size while TBA$^+$ system gave ZSM-11 (MEL).

Shantz *et al.* (1998) used solid-state NMR to study the dynamic of organic molecule (N,N,N-trimethyl alkylammonium cations; alkyl = isopropyl, cyclopentyl, cyclohexyl, or norbornyl) occluded in the as-synthesized high-silica tectosilicate nonasile. It was found that the steric confinement the nonasile cage exerted on the larger (Cn>C5) substituent alkyl groups, which indicated strong organic-inorganic interaction. For aluminosilicate synthezed with charged structure-directing agents, strong organic-inorganic interaction might allow for aluminum preferentially occupying specific framework sites. This could lead to tailoring the distribution of

catalytic sites in zeolites base on the charge distribution of the structure-direction agent.

Gittleman *et al.* (1996) also used N,N,N-trimethyl-1-adamantammonium cation as template and found that in the presence of potassium cation, SSZ-24 was formed while in the presence of sodium cation, the SSZ-31 was firstly produced. While in the system of rubidium or cesium caitons, the unknown silicate was obtained.

Zones *et al.* (1996) used high rigid polycyclic hydrocarbons (a family of related quaternary ammonium derivatives of tricyclodecane hydrocarbon) as charged derivatives. They occupy space in order to developing guest/host zeolite lattices. It was found that for organo-cations, the steric requirements appeared to be the most important feature in determining phase selectivity. Moreover, at high pH values, aluminate was less soluble and therefore crystallization of aluminosilicate was favored. Relating to the gel chemistry leading to the final host lattices the organic chemistry of the guest organo-cation and inorganic factors affected the product selectivity. At too high alkali concentration in the synthesis, the use of the tricyclodecane family as guest molecule or template gave Mordenite and SSZ-13 (a synthetic chabazite) as major products. At lower alkali metal levels and lower alkalinity, the individual tricyclodecane organo-cations showed much greater selectivity in terms of zeolites produced.

Crown ethers are also selected for using as structural directing agent. Chatelain *et al.* (1995) used 18-crown-6 ether as organic template in synthesizing RHO type zeolite. A reduction in Na_2O content of the starting mixture also led to highly crystalline products and enhanced the framework Si/Al ratio. RHO type showed no framework distortion upon dehydration by heating due to a higher covalent characteristic of the silica rich framework bonds, which enhanced its rigidity. In 1996, they also used the same template in synthesizing KFI type zeolite at Si/Al ratio > 4.0. The crystalline started to occur at $K_2O/Al_2O_3 > 1.8$.

Dougnier *et al.* (1996) used both 16-crown-5 and 18-crown-6 ethers for FAU and EMT type zeolite synthesis. Removing crown ether can be done by heating in solution containing a protonated amine or quaternary ammonium salt. This method

is seemingly based upon the ion exchange of the crown ether/Na$^+$ complex and the charged amine compound.

According to previous works, beside successfully using as structural directing agent, alkyamine and polyalkyamine also incorporate into the zeolite framework causing charge-balancing protonated amine and lowering in Na content (Na/Al < 1). Crown ethers also create the same phenomena. However, removing crown ethers by exchanging with protonated amine or quaternary ammonium salt also has organic remained in framework.

Concerning with inorganic components, three factors must be considered. The concentration of trivalent element affects to the capable of substituting for silicon lattice while hydroxyl anion can dominate the silicate chemistry, thereby playing a critical role in determining what product is formed. Alkaline cations can also act as template and dominate the course of crystallization. The role of organic components, as well as structural direction agent, increase flocculating stability due to the formation of stable organic-inorganic micelle (self-assmebling) as intermediate formation of mesostructured material. This formation reduces film drainage and coalescence. Moreover, the preparative chemistry of ordered mesoporous solids, closely bounds to colloid chemistry accelerating framework formation.

This concept brought out the using of metal alkoxide precursors. Besides, they are easily removed from the solution and not participated in subsequent processes, metal alkoxides are greatly useful to be used as metal oxide-precursors. In general, alkoxides are thermodynamically unstable in aqueous solution. They usually react readily with water to form precipitates, however, the hydrolytic rate depends on the size of the organic parts (steric effect) and the number of hydroxyl groups in the ligand (chelate or cage effect). Moderate alkoxide reactivity towards the nucleophilic attack of water is a necessary requirement for their applicability as precursors of gels or mesostructured material formation. The selection of the series of functionalized polyalcohols to construct adequate precursor is thus very important.

Cabrera *et al.* (2000) purposed the use of atrane, atrane complexes and atrane derivative of B, Al, Si, Ti, Zr, and etc. as precursor for both non-siliceous and mix-

oxide mesostructure and mesoporous system. Triethanolamine (TEA) was selected as an alkoxide bidentate ligand, due to their ability in forming amine-trialkoxo complexes (with a diversity of elements) by action as anionic (tetradentate) tripod ligand and cetyltrimethylammonium bromide (CTAB) was used as surfactant directing agent. Their work indicated that the final ordered mesoporous materials were thermally stable and showed unimodal porosity as well as homogenous microstructure and texture. However, the final products can't go forward as mesoporous solid or crystalline aluminosilicate because the remaining organic portions hindered the formation of the wanted continuous oxide network. For mixed element system, the results showed that the incorporate of Al leaded to increasing disorder because of hexagonal disordering of pore packing motif and decreased pore sizes, whereas the pore wall thickness continuously increased.

As a summary, quarternary amonium cations and bulky cyclic organics used remain in the framework, while small amines can stay in the framework and act as counter ion in the place of sodium ion. Linear polyamines usually decompose into ammonium ion and also act as counter ion in the framework. Synthesizing without organic part usually precipitate the crystals soon right after nucleation, causing secondary nucleation in the system and providing wide distribution of particle size. In order to maintain the particles in the crystallization growth state, flocculating in the solution, the organic content in the gel state system is necessary. Using atranes as metal alkoxide precursors is new and very interesting. Even it did not go forward to mesoporous solid as stated in Cabrera et. al.'s work due to the organic portions hindered the metal oxide framework formation.

1.3 Objectives

This work has been planned to use synthesized atranes (silatrane and alumatrane) as zeolite synthesis precursors using sol-gel process followed by hydrothermal treatment and alkaline base as hydrolysis agent and source of metal ions in the absence of surfactant. The parameters studied in this work are aging temperature and time, precursors loading ratio, type and concentration of alkali metals.